

Frost and drought: Effects of extreme weather events on stem carbon dynamics in a Mediterranean beech forest

Ettore D'Andrea¹  | Negar Rezaie^{1,2}  | Peter Prislan³  | Jozica Gričar³  |
Alessio Collalti^{4,5}  | Jan Muhr^{6,7}  | Giorgio Matteucci^{1,8} 

¹National Research Council of Italy, Institute for Agriculture and Forestry Systems in the Mediterranean (CNR-ISAFOM), Ercolano, Naples, Italy

²Consiglio per la Ricerca in Agricoltura e l'Analisi dell'Economia Agraria, Centro Ricerca Ingegneria e Trasformazioni Agroalimentari (CREA-IT), Monterotondo Scalo, Rome, Italy

³Slovenian Forestry Institute, Ljubljana, Slovenia

⁴National Research Council of Italy, Institute for Agriculture and Forestry Systems in the Mediterranean (CNR-ISAFOM), Perugia, Perugia, Italy

⁵Department of Innovation in Biological, Agro-food and Forest Systems, University of Tuscia, Viterbo, Italy

⁶Bioclimatology, University of Göttingen, Göttingen, Germany

⁷Department of Biogeochemical Processes, Max-Planck-Institute for Biogeochemistry, Jena, Germany

⁸Institute for BioEconomy (CNR-IBE), National Research Council of Italy, Sesto Fiorentino, Florence, Italy

Correspondence

Ettore D'Andrea and Negar Rezaie, National Research Council of Italy, Institute for Agriculture and Forestry Systems in the Mediterranean (CNR-ISAFOM), via Patacca 2, 80056 Ercolano, NA, Italy.
Email: ettore.dandrea@cnr.it (E. D.) and rezaie.negar@gmail.com (N. R.)

Funding information

eLTER H2020 Project, Grant/Award Number: 654359; Italian Ministry of University and Research, Grant/Award Numbers: CNR DBA. AD003.139, CNR DTA.AD003.474; National Research Council of Italy, Department of Biology, Agriculture, and Food Secures, Grant/Award Number: 71951

Abstract

The effects of short-term extreme events on tree functioning and physiology are still rather elusive. European beech is one of the most sensitive species to late frost and water shortage. We investigated the intra-annual C dynamics in stems under such conditions. Wood formation and stem CO₂ efflux were monitored in a Mediterranean beech forest for 3 years (2015–2017), including a late frost (2016) and a summer drought (2017). The late frost reduced radial growth and, consequently, the amount of carbon fixed in the stem biomass by 80%. Stem carbon dioxide efflux in 2016 was reduced by 25%, which can be attributed to the reduction of effluxes due to growth respiration. Counter to our expectations, we found no effects of the 2017 summer drought on radial growth and stem carbon efflux. The studied extreme weather events had various effects on tree growth. Even though late spring frost had a strong impact on beech radial growth in the current year, trees fully recovered in the following growing season, indicating high resilience of beech to this stressful event.

KEYWORDS

climate change, *Fagus sylvatica* L. (beech), growth, phenology, resilience, wood formation

1 | INTRODUCTION

Tree stems play an important role in the carbon balance of forest ecosystems (Yang, He, Aubrey, Zhuang, & Teskey, 2016). Part of the carbon (C) fixed by photosynthesis is allocated to the stem, some is respired by stems and emitted into the atmosphere as CO₂, and a minor part is released as volatile organic compounds (Rissanen, Vanhatalo, Salmon, Bäck, & Hölttä, 2020). Radial growth—an often used proxy for the overall allocation of C to the stem (Bascietto, Cherubini, & Scarascia-Mugnozza, 2004; Chan, Berninger, Kolari, Nikinmaa, & Hölttä, 2018; Cuny et al., 2015)—is largely related to the process of wood formation, which can be divided into five (main) developmental phases: (a) cambial cell division; (b) cell enlargement; (c) secondary wall deposition and (d) cell wall thickening (lignification), while (e) in the case of vessels and fibres, also genetically-programmed cell death or *apoptosis* (Prislan, Čufar, De Luis, & Gričar, 2018). The whole process is known to be sensitive to many factors, such as leaf phenology (Michelot, Simard, Rathgeber, Dufrêne, & Damesin, 2012), temperature (Begum, Nakaba, Oribe, Kubo, & Funada, 2007), drought (Linares, Camarero, & Carreira, 2009), tree-size and social status (Rathgeber, Rossi, & Bontemps, 2011) and tree vigour (Gričar, Krže, & Čufar, 2009).

A recent global estimate (Yang et al., 2016) showed that the stem CO₂ efflux (ES) alone, from boreal to tropical forests combined, was 6.7 (±1.1) Pg C year⁻¹, accounting for 11% and 20% of global forest ecosystem gross primary production and net primary production, respectively. However, accurate field measurements of actual stem respiration (RS) are difficult if not impossible (Teskey, Saveyn, Steppe, & McGuire, 2008), and the most commonly measured proxy, stem CO₂ efflux (ES), is likely to underestimate local respiration (Trumbore, Angert, Kunert, Muhr, & Chambers, 2013). For example, ES was found to vary between 82–94% and 86–91% of RS in *Populus deltoides* W. Bartram ex Marshall (Saveyn, Steppe, Mc Guire, Lemeur, & Teskey, 2008) and *Dacrydium cupressinum* Lamb stems (Bowman et al., 2005), respectively. Lower values (up to 45%) were observed applying the mass balance approach (Teskey & McGuire, 2007) and using the O₂ uptake technique, as an alternative proxy for actual respiration (up to 41%, Hilman et al., 2019). ES and RS are different because part of the CO₂ produced by respiration is not released directly through the bark into the atmosphere, but is dissolved in xylem sap and is carried upward by the transpiration stream (Bloemen et al., 2014). In addition, ES is affected by CO₂ deriving from root respiration, which is also carried upward into the stem (Bloemen, McGuire, Aubrey, Teskey, & Steppe, 2013). Moreover, part of respired CO₂ can be fixed in xylem storage pools (DeRoo, Salomón, & Steppe, 2020). ES is influenced by many factors, such as air temperature (Yang et al., 2016), growth rate (Damesin, Ceschia, le Goff, Ottorini, & Dufrêne, 2002), distribution and turnover of living cells (Collalti et al., 2020) and tree social status (Guidolotti, Rey, D'Andrea, Matteucci, & de Angelis, 2013). RS can be separated in growth respiration (R_G), which provides the energy for synthesizing new tissues; and by maintenance respiration (R_M), which maintains existing living cells (Amthor, 2000; Thornley, 1970). Separating RS into these

components, which are partly included in ES, allows further investigation of stem carbon budgeting and tissue costs (Chan et al., 2018).

Even small changes in the mean or variation of a climate variable may cause disproportionately large changes in the frequency of extreme weather events, recognized as major drivers of current and future ecosystem dynamics (Frank et al., 2015). In the near future, the Mediterranean region is predicted to be the most vulnerable of the European regions to global change (Schröter et al., 2005). Changes in temperature and precipitation regimes may increase drought risk, which can negatively affect physiological performance (Rezaie et al., 2018), carbon allocation (D'Andrea, Guidolotti, Scartazza, De Angelis, & Matteucci, 2020), as well as the growth and competition strength (Peuke, Schraml, Hartung, & Rennenberg, 2002) of common beech, one of the most important and widespread broadleaved trees in Europe. Increasing spring temperatures can trigger earlier leaf unfolding (Allevato et al., 2019; Gordo & Sanz, 2010), which in turn results in a higher risk that young leaves are exposed to late spring frost (Augsburger, 2013), especially in Europe (Zohner et al., 2020) and at higher elevations (Vitasse, Schneider, Rixen, Christen, & Rebetez, 2018). Temperatures below −4°C can kill the developing new shoots and leaves, thus reducing the photosynthetic area and ultimately the trees' growth. In the case of late frost, depending on the intensity of damage, the formation of new leaves requires a high amount of reserves (D'Andrea et al., 2019; Dittmar, Fricke, & Elling, 2006). Despite the crucial role of extreme events and increasing attention on their prospective increasing role in future climate scenarios, information on the effect of short-term extreme events on tree functioning is still fairly elusive (Carrer, Brunetti, & Castagneri, 2016; Gazol et al., 2019). In this respect, not much is known about the interaction between wood formation (i.e., xylogenesis) and ES. At the seasonal timescale, the capacity of stem micro-coring technique to identify phenological phases of wood formation allows to attribute metabolic costs to each one of them (Meir, Mencuccini, & Coughlin, 2019). A deeper investigation of this link is crucial, especially in the context of climate change, associated with increased frequency of extreme weather events (e.g., drought and late frost), which may greatly modify the contribution of these processes to the C cycle and their effect on tree performance. In this context, we monitored xylogenesis, together with ES and overall growth, in a mature Mediterranean beech forest (*Fagus sylvatica* L.) from 2015 to 2017—a period characterized by a spring late frost (2016) and a summer drought (2017)—with the objective of unravelling the intra-annual C dynamics in stems under different climatic conditions and in response to extreme weather events. On the hypothesis that extreme weather events would alter the stem C dynamics at both tree and stand scales, we investigated tree scale physiological processes specifically, of growth (xylogenesis) and respiration (proxied by stem CO₂ efflux), and then up-scaled to stand-scale growth and C emission related to this process. We hypothesized that: (a) cambial activity and radial growth may have ceased soon after leaf death due to the 2016 spring late frost; (b) second leaf re-sprouting starts at the expense of stem growth; (c) the 2017 summer drought would have negatively impacted stem biomass production and effluxes and that (d) climatic variability

and extreme weather events are important factors in C dynamics on tree and stand scales.

2 | MATERIALS AND METHODS

2.1 | Study site

The measurements were carried out between 2015 and 2017 in a long-term monitored beech stand (*Fagus sylvatica* L.) located at Selva Piana (41°50'58" N, 13°35'17" E, 1,560 m elevation), close to Collelongo (Abruzzi Region, Italy) in the Central Apennines. The site, established in 1991 and since 2006 part of the long-term ecological research (LTER) network, is located in a 3,000 ha forest included in the wider forest area of the external belt of Abruzzo-Lazio-Molise National Park. In 2017, the stand density was 725 trees ha⁻¹, the basal area was 45.77 m²/ha with a mean diameter at breast height (DBH) of 28.5 cm and a mean tree height of 23 m. In 2013, mean tree age was estimated to be about 110 years. The site topography is gently sloping and the soil is humic alisol with a variable depth (40–100 cm), developed on calcareous bedrock. The climate is of Mediterranean mountain type, during the period 1989–2014 the mean annual temperature was 7.2°C, and the mean annual precipitation was 1,178 mm, of which ~10% falls in summer (Collalti et al., 2016; Guidolotti et al., 2013; Reyer et al., 2020).

2.2 | Tree selection, wood formation dynamics, xylem phenology and C fixation

Sampling was performed on five trees, as done in other studies on wood formation and stem CO₂ efflux (e.g., Ceschia, Damesin, Lebaube, Pontailler, & Dufrene, 2002; Damesin et al., 2002; Gruber, Wieser, & Oberhuber, 2009; Delpierre et al., 2019), with a mean (±SE) age of 109 ± 4 years and mean DBH of 47.5 ± 1.7 cm. Trees were selected for their similarity (*sensu* Gleichläufigkeit, GLK 70–85, which measures the percentage of common signs of year-to-year growth change between two series) with the site tree ring chronology (Expressed Population Signal = 0.89) as in Rezaie et al. (2018). We followed this approach because of the applied method for stem CO₂ efflux measurement, which needs big trees to allow fixing of collars. Hence, selected trees were larger than the average of stand trees, but still representative of the site growth pattern. Microcore collection and ES measurements were carried out from April 2015—that is, before leaf unfolding—until November 2017, when the trees had completely lost their leaves. Microcores (2 mm diameter and 15 mm long each) were extracted from each tree at 1.1–1.7 m above ground using a Trepbor tool (Rossi, Menardi, Fontanella, & Anfodillo, 2005). Microcores were collected 15, 12 and 14 times in 2015, 2016 and 2017, respectively. To avoid wound effects, cores were sampled at a distance of at least 5 cm from each other. The microcores, containing bark, cambium, newly developing xylem and one to two older xylem rings, were immediately stored in formaldehyde–ethanol–acetic acid solution in the field. Cross sections of the microcores were prepared

following the standard methodology (Prislan, Gričar, de Luis, Smith, & Cufar, 2013) and were photographed in high definition under a Leica DM 4000 microscope (Leica Microsystems, Wetzlar, Germany) using transmission and polarized light. Histometrical analyses were performed on images taken with a Leica DFC 280 digital camera using the Leica Application Suite image analysis system (Leica Microsystems, Germany). On each photographed cross section, the number of cambium cells was counted and the widths of the developing xylem were measured along three parallel lines (Figure 1).

The dynamics of xylem formation were analysed by fitting the Gompertz function to xylem increments (Prislan et al., 2018; Rathgeber, Santenoise, & Cuny, 2018), corrected for the width of the previous tree ring to reduce the effect of the sampling position (Camarero, Guerrero-Campo, & Gutierrez, 1998; Oladi, Pourtahmasi, Eckstein, & Bräuning, 2011), as follows:

$$y = \alpha \exp \left[-e^{(\beta - kt)} \right] \quad (1)$$

where y is the cumulative ring width (μm) at time t (day of the year), α is the final asymptotic size representing the annual potential growth, β is the x-axis placement parameter and k is the rate of change parameter.

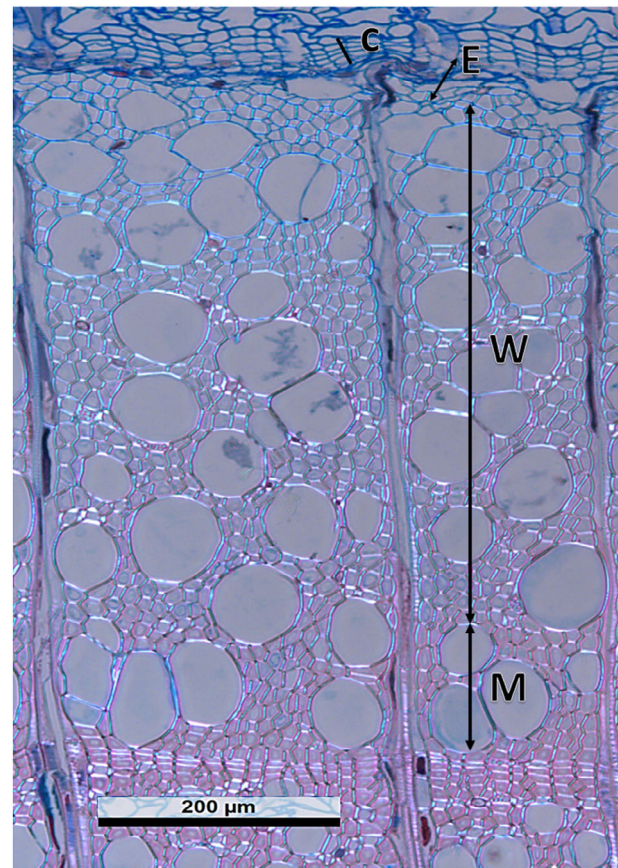


FIGURE 1 Transverse section of a sample (July 15, 2015) under polarized light microscopy: cambium (C), enlarging cells (E), wall thickening cells (W), mature cells (M) [Colour figure can be viewed at wileyonlinelibrary.com]

For each tree and monitoring year, the following phenological xylem formation phases were recorded: (a) cambium *reactivation*, (b) beginning of cell *enlargement* (bE); (c) beginning of cell wall *thickening* (bW); (d) beginning of cell *maturation* (bM); (e) *cessation* of cell enlargement (cE) and (f) *cessation* of cell wall thickening and *lignification* (cW). The date of cambium reactivation was assessed as the average between dates when an increase of cambium cells was observed (i.e., from 3–4 to 6–7 cells in a radial row) (Čufar, Prislan, de Luis, & Gričar, 2008; Deslauriers, Rossi, Anfodillo, & Saracino, 2008). Phases of xylem growth and ring formation were computed using logistic regression, spanning from the 50% probability that phenophases have started or ended (Rathgeber et al., 2018). Based on phenological phases, the durations of key wood formation phases were calculated: (a) the overall duration of the enlargement period ($dE = cE - bE$); (b) the duration of the wall-thickening period ($dW = cW - bW$) and (c) the total duration of wood formation (i.e., the duration of xylogenesis) ($dX = cW - bE$). Data were analysed using the CAVIAR (v2.10-0) package (Rathgeber et al., 2018) built for R statistical software (R Development Core Team, 2018).

In April 2015, DBH of each sampled tree was measured using a dendrometric tape, and annual DBH increment in the measurement period was obtained through tree microcores analysis. The annual C fixed in the stem (SG_t) was estimated for each of the sampled tree, as follows:

$$SG_t = \frac{0.46 \times (BS_t - BS_{t-1})}{\Delta t} \quad (2)$$

where SG_t is the amount of C fixed in the stem per year expressed in Mg C year⁻¹, 0.46 is the carbon content of the woody tissue measured at the site (Scarascia-Mugnozza, Bauer, Persson, Matteucci, & Masci, 2000), BS_t and BS_{t-1} are the stem biomass in Mg dry matter (DW) at the beginning and at the end of each sampling year and Δt is the time variation (1 year).

The site-specific allometric equation for beech used for BS was that proposed by Masci (2002):

$$BS = \frac{283.734 \times DBH^{2.134}}{10^6} \quad (3)$$

where BS is in Mg DW, and DBH (in cm) is the stem DBH (1.30 m) ($R^2 = .96$, p -value < .01).

Up-scaling to stand scale was performed according to the following equation:

$$SG = SG_t \times \frac{BA}{CS_{st}} \quad (4)$$

with SG expressed in Mg C ha⁻¹ year⁻¹, BA is the stand basal area (m² ha⁻¹) and CS_{st} (m²) is the cross-sectional area of individual trees at 1.30 m.

2.3 | Stem CO₂ efflux (ES)

On the same trees monitored for wood formation, two PVC collars (10 cm diameter and 5 cm high, one facing north and one south) were fixed with flexible plastic ties and sealed leak tight with Terostat, a CO₂ neutral paste (Henkel KgaA, Germany). When present, bark mosses and lichens were removed. Stem CO₂ efflux was measured with a portable IRGA (EGM 4, PP-System, Hitchin, UK), equipped with a closed-dynamic chamber (SRC-1, PP-System), which was tightened (Figure S1). On a singular collar, each measurement consisted of a 120-s loop, in which the CO₂ concentration inside the chamber was measured every 5 s. During measurements, the CO₂ concentration typically increased by 10–50 μmol mol⁻¹. Stem CO₂ efflux (ES) was calculated as:

$$ES = K_{CO_2} \div V_{mol} \times \frac{V_{cuV}}{A} \quad (5)$$

where ES is the stem CO₂ efflux per unit surface area (μmol m⁻² s⁻¹), K_{CO_2} (μmol mol⁻¹ s⁻¹) is the slope of the regression between CO₂ concentration and time during measurements, while V_{mol} , the molar volume, is the volume occupied by 1 mol of CO₂ (m³/mol), at the air pressure (measured by the sensor built-in the EGM-4 soil respiration analyser) and air temperature (T_{air} in °C) at the measurement time, A is the exposed lateral surface area of the stem (m²) and V_{cuV} is the sum of the SRC-1 cuvette (Figure S1) and collar volumes (m³).

Stem CO₂ efflux was measured 15, 12 and 11 times in 2015, 2016 and 2017, respectively. Measurements were always performed in the late morning starting between 10:30 a.m. and 12:00 p.m., and the overall sampling time was around 40 min.

An exponential function was used to assess the seasonal relationship between ES and T_{air}

$$ES = a \times e^{T_{air} \times b} \quad (6)$$

and ES overall temperature sensitivity for a 10°C increase (Q_{10}) was calculated as:

$$Q_{10} = e^{10 \times b} \quad (7)$$

where b is derived from Equation (6).

Considering the wood formation duration ($dX = cW - bE$) as the difference between the end of the wall thickening phase (cW) and the beginning of the enlargement phase (bE) (see paragraph Section 2.2), we identified for each tree the wood formation period, when both maintenance and growth respirations occur (mg), and non-wood formation periods, when only the maintenance respiration is active (m), making it possible to divide the measured ES into two groups. According to Equation (5), we calculated for each group the specific CO₂ efflux at a base air temperature of 15°C (ES_{15mg} and ES_{15m}) and the specific Q_{10} (Q_{10mg} and Q_{10m}).

According to the mature tissue method (Amthor, 2000; Thornley, 1970), during the non-wood formation period, ES_m

($\mu\text{mol m}^{-2} \text{s}^{-1}$) was constituted only by the effluxes derived by maintenance respiration, which was calculated as:

$$ES_m = ES_{15m} \times Q_{10m}^{\frac{(T_{\text{air}}-15)}{10}} \quad (8)$$

During the wood formation period, ES_{mg} ($\mu\text{mol m}^{-2} \text{s}^{-1}$), which is affected by both maintenance and growth respiration, was calculated as:

$$ES_{\text{mg}} = ES_{15\text{mg}} \times Q_{10\text{mg}}^{\frac{(T_{\text{air}}-15)}{10}} \quad (9)$$

According to Thornley (1970) and Rodríguez-Calcerrada et al. (2019), ES_m and its relationship with air temperature was assumed to be also valid during the wood formation period, although this approach does not account for the acclimation of maintenance respiration to temperature during warmer periods (Collalti et al., 2018, and references therein). However, there are contrasting hypotheses on the magnitude of acclimation (Carey, Callaway, & DeLucia, 1997; Stockfors & Linder, 1998). Under the above-mentioned assumptions, we calculated the stem CO_2 efflux due to growth respiration, ES_g ($\mu\text{mol m}^{-2} \text{s}^{-1}$), as:

$$ES_g = ES_{\text{mg}} - ES_m \quad (10)$$

The daily CO_2 effluxes of the whole stem were obtained by integrating, over the entire stem area, the effluxes through Equations (7)–(9), using half-hourly T_{air} values measured at the site.

The stem area was calculated as follows:

$$LS = 0.464 \times \text{DBH} - 2.083 \quad (11)$$

where LS is the stem lateral surface (m^2) ($R^2 = .828$, p -value $< .01$, for more details on the equation see additional material Methods S1, Figures S2 and S3). Using DBH, we considered the measurement at 1.30 m to be representative of the whole stem, even though contrasting effects of height on stem CO_2 effluxes have been reported (e.g., Damesin et al., 2002; Katayama, Kume, Ichihashi, & Nakagawa, 2019).

Daily stem CO_2 effluxes ($\mu\text{mol CO}_2 \text{ tree}^{-1} \text{ day}^{-1}$) were converted in daily C effluxes ($\text{g C tree}^{-1} \text{ day}^{-1}$) multiplying the moles of CO_2 for C molar mass (12 g/mol^1).

Annual values of the C effluxes of the five sampled trees (TES_{mg} , TES_m , TES_g , $\text{g C tree}^{-1} \text{ year}^{-1}$, see Table 1 for definitions) were obtained by summing up the daily values.

On the assumption that the selected trees were representative of the stand, annual values of each of the fluxes at stand scale (AES_{mg} , AES_g and AES_m , all in $\text{Mg C ha}^{-1} \text{ year}^{-1}$, see Table 1 for definitions) were calculated as:

$$AES_x = 10^{-6} \times TES_x \times \frac{BA}{CS_{\text{st}}} \quad (12)$$

where TES_x was the effluxes at tree level (TES_{mg} , TES_g and TES_m), BA is the stand basal area ($\text{m}^2 \text{ ha}^{-1}$) and CS_{st} (m^2) is the cross-sectional area of individual trees at 1.30 m.

TABLE 1 List of terms used in the text

Terms	Definition	Spatial scale
ES	Stem CO_2 efflux per surface area ($\mu\text{mol m}^{-2} \text{s}^{-1}$)	Local
ES_{15w}	Specific CO_2 efflux at an air temperature of 15°C during the wood formation period ($\mu\text{mol m}^{-2} \text{s}^{-1}$)	Local
ES_{15m}	Specific CO_2 efflux at an air temperature of 15°C during the non-wood formation period ($\mu\text{mol m}^{-2} \text{s}^{-1}$)	Local
$Q_{10\text{mg}}$	ES temperature sensitivity for a 10°C increase during the wood formation period	Local
Q_{10m}	ES temperature sensitivity for a 10°C increase during the non-wood formation period	Local
ES_{mg}	Stem CO_2 efflux per surface area ($\mu\text{mol m}^{-2} \text{s}^{-1}$) during wood formation	Local
ES_m	Stem CO_2 efflux per surface area ($\mu\text{mol m}^{-2} \text{s}^{-1}$) due to maintenance respiration	Local
ES_g	Stem CO_2 efflux per surface area ($\mu\text{mol m}^{-2} \text{s}^{-1}$) due to growth respiration	Local
TES_{mg}	Annual stem C efflux (g C year^{-1})	Tree
TES_m	Annual stem C efflux due to maintenance respiration (g C year^{-1})	Tree
TES_g	Annual stem C efflux due to growth respiration (g C year^{-1})	Tree
AES_{mg}	Annual stem C efflux ($\text{Mg C ha}^{-1} \text{ year}^{-1}$)	Stand
AES_m	Annual stem C efflux due to maintenance respiration ($\text{Mg C ha}^{-1} \text{ year}^{-1}$)	Stand
AES_g	Annual stem C efflux due to growth respiration ($\text{Mg C ha}^{-1} \text{ year}^{-1}$)	Stand
SG	Annual C fixed in stem biomass ($\text{Mg C ha}^{-1} \text{ year}^{-1}$)	Stand

2.4 | Meteorological and phenological data

For the period 1989–2014, FLUXNET2015 data release was used for half-hourly air temperature and precipitation (Pastorello et al., 2020; Reyer et al., 2020). For the study period (2015–2017), measured data were gap filled using downloaded data by the ERA5 database of the European Centre for Medium-Range Weather Forecasts (ECMWF) (<https://www.ecmwf.int/en/forecasts/datasets/archive-datasets/reanalysis-datasets/era5>), according to FLUXNET 2015 release equations.

The Standardized Precipitation Evapotranspiration Index (SPEI), considered the most appropriate index for the Mediterranean climate (Vicente-Serrano et al., 2013), was used to assess the magnitude of the drought in 2017. This index is based on the difference between precipitation and potential evapotranspiration (PET), computed according to Hargreaves' equation. The 3-month SPEI was calculated for the site for the period 1989–2017, using the SPEI package in R.

Soil water content was measured at the site under the litter and at depths of 0.05, 0.20 and 0.50 m in the soil by four permanent sensors using the Time Domain Reflectometry technique (CS-616, Campbell Scientific, Logan, UT). Measurements were performed with 20 s frequency and averaged over half hour.

Leaf phenology was monitored using the MODIS leaf area index (LAI) product (MOD15A2H, <https://modis.gsfc.nasa.gov/>) with 8-day temporal resolution and 500-m spatial resolution. The date of onset of photosynthetic activity (green up) and the date at which plant green leaf area peaked its annual maximum (maturity) were assessed through the rate of change in the curvature of the fitted logistic models (Zhang et al., 2003).

2.5 | Statistical data analysis

Descriptive parameters of growth and xylem phenology were tested using one-way repeated measures analysis of variance, with years as predictive factor, followed by the Holm–Sidak post hoc method. Linear mixed models, considering “tree” and “sampling date” as crossed random effects, were used to account for the random variation of the ES inter-annual measurements. An exponential equation was used to evaluate the relationship between ES and T_{air} . Differences among ES parameters (Q_{10} and ES_{15}) were tested using two-way repeated measures analysis of variance (two factors repetition), using year and period (non-wood formation, wood formation) as predictive factors. Multiple comparisons were performed by the Holm–Sidak method. Linear regressions were used to assess the relationship between tree ring widths (TRW) and mean annual ES. We tested data normality and constant variance using the Shapiro–Wilk test and the Spearman rank correlation between the absolute values of the residuals and the observed value of the dependent variable.

3 | RESULTS

3.1 | Description of extreme weather events

In the night between the April 25 and 26, 2016 (day of year, DOY 115), a spring late frost occurred in Central and Southern Italy, causing leaf damage in many beech stands (Allevato et al., 2019; Bascietto, Bajocco, Mazzenga, & Matteucci, 2018; Greco et al., 2018; Nolè, Rita, Ferrara, & Borghetti, 2018). At the Selva Piana site, the air temperature reached -6°C at canopy level, destroying the whole-stand canopy (Figure 2) and leaving the trees without leaves for almost 2 months (Bascietto et al., 2018; D'Andrea et al., 2019).

In the summer of 2017, a positive temperature anomaly affected Central Italy and the Balkans, with a duration ranging from 20 to 35 days (Rita et al. 2020). In the same year, annual precipitation was 950 mm (while the 1989–2014 average was $1,136 \pm 40.8$ mm), with only 54 mm of precipitation throughout the entire summer (while the 1989–2014 average was 183 ± 13.9 mm). In August 2017, the site experienced only 1 mm of rain (while the 1989–2014 average was

50.7 ± 8.6 mm), with an average maximum air temperature of 23.9°C , about 3°C warmer than the long-term 1989–2014 average ($20.8 \pm 0.3^{\circ}\text{C}$). Such particular weather conditions led to a summer SPEI < 1.5 (Figure 3) and to a soil water content (SWC, daily mean of the measurement at 5 and 20 cm depth) of 0.22 ± 0.01 m/m. This value is lower ($F = 45.935$, p -value = $<.001$) than 0.28 ± 0.01 and 0.31 ± 0.02 m/m assessed in 2015 and 2016, respectively.

3.2 | Wood formation dynamics and leaf phenology

The date of onset of photosynthetic activity, based on LAI dynamics, differed among the study years, occurring at DOY 118, 95 and 127 in 2015, 2016 and 2017, respectively. The second leaf unfolding, occurred after the 2016 late frost, did not lead to a second wood formation cycle. In all 3 years, cambium reactivation occurred after leaf unfolding at DOY 123 ± 4 , 118 ± 8 and 138 ± 6 in 2015, 2016 and 2017, respectively (Figure 4). In 2016, cambium cell production also continued after the late frost event, but at considerably lower rates. Different intra-annual growth patterns were observed during the three study years, especially in the year of the late frost (2016, Figure 5a, Table 2).

In 2016, the maximum growth rate (rx) ($F = 8.469$, p -value = .014) was lower and was reached 3 weeks earlier (tx) ($F = 22.667$, p -value $<.001$) than in the other 2 years. The different intra-annual growth patterns also resulted in significantly narrower tree rings in 2016 (230.12 ± 1.54 μm) ($F = 13.272$, p -value $<.01$) than in 2015 ($1,312.17 \pm 196.15$ μm) and 2017 ($1,234.80 \pm 269.32$ μm).

Differences were also observed for the beginning, cessation and duration of wood formation phases (Figure 5b). The beginning of the enlargement phase occurred earliest in 2016 and latest in 2017 ($F = 34.789$, p -value $<.001$). The cessation of this phase was anticipated in 2016 ($F = 17.155$, p -value $<.01$). Consequently, the duration of the enlargement phase was longer in 2015 (110 ± 22 days) than in 2016 (82 ± 4 days) and 2017 (78 ± 4 days) ($F = 8.025$, p -value = .01).

The beginning of the wall thickening phase did not differ among the years ($F = 4.188$, p -value = .06). The cessation of this phase occurred earlier in 2016 ($F = 69.167$, p -value $<.001$). The duration of the wall thickening phase was thus shorter in 2016 (57 ± 5 days) than in 2015 (99 ± 6 days) and 2017 (75 ± 4 days) ($F = 26.561$, p -value $<.001$). We also observed a delay in the beginning of cell maturation in 2016 (at DOY 200 ± 4) with respect to 2015 (at DOY 178 ± 4) and 2017 (at DOY 176 ± 2) ($F = 11.650$, p -value $<.01$). The overall duration of wood formation was longer in 2015 (128 ± 5 days) than in 2016 (98 ± 8 days) and 2017 (97 ± 8 days) ($F = 12.561$, p -value $<.001$).

3.3 | Stem CO₂ efflux

During the monitoring period (April 2015–November 2017), the measured ES ranged between 0.16 ± 0.03 $\mu\text{mol CO}_2 \text{ m}^{-2} \text{ s}^{-1}$ (December

FIGURE 2 Selva Piana forest (Collelongo, Abruzzi region) photographed the May 19, 2016, 24 days after the late frost [Colour figure can be viewed at wileyonlinelibrary.com]

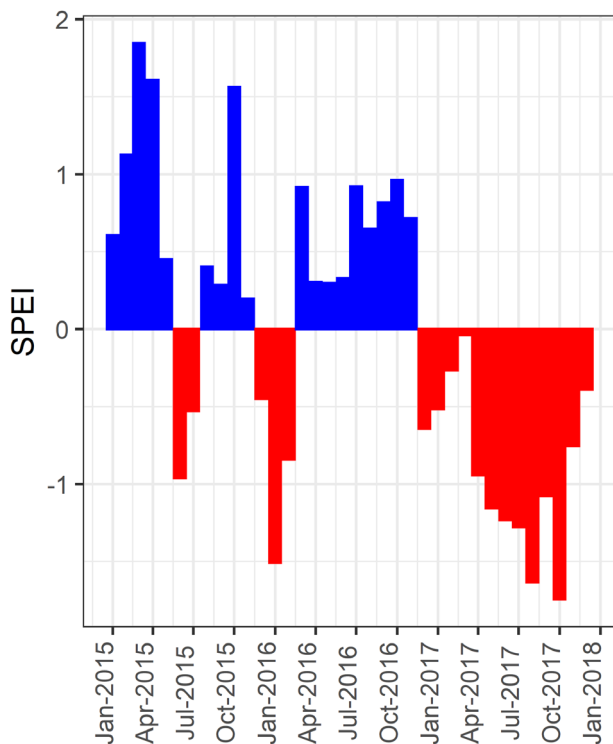


FIGURE 3 Three-month Standardized Precipitation Evapotranspiration Index (SPEI) at the experimental site of Selva Piana-Collelongo in 2015, 2016 and 2017 [Colour figure can be viewed at wileyonlinelibrary.com]

2015) and $3.01 \pm 0.40 \mu\text{mol CO}_2 \text{ m}^{-2} \text{ s}^{-1}$ (August 2017) (Figure 6). Mean ES measured in 2016 ($0.68 \pm 0.19 \mu\text{mol CO}_2 \text{ m}^{-2} \text{ s}^{-1}$) was lower ($F = 24.476$, p -value $< .01$) than in 2015 ($1.11 \pm 0.40 \mu\text{mol CO}_2 \text{ m}^{-2} \text{ s}^{-1}$) and 2017 ($1.29 \pm 0.30 \mu\text{mol CO}_2 \text{ m}^{-2} \text{ s}^{-1}$). Results from the linear mixed model showed that trees and sampling dates account for 11 and 75% of the total variance of ES, respectively.

In each year, ES was strongly related to air temperature through the standard exponential function (Figure 7). The relation was

confirmed at different aggregation levels of measurements (whole year, wood formation and non-wood formation periods; see also Table S1 in Supporting Information).

Considering the non-wood and wood formation period, average Q_{10} was 2.75 ± 0.15 , 2.11 ± 0.18 and 2.68 ± 0.15 , in 2015, 2016 and 2017, respectively (Table S1 in Supporting Information). The Q_{10} parameter was not strongly affected by the sampling year (p -value = .059), although the values in 2016 were 22% lower than in the other 2 years. Wood formation affected the Q_{10} parameter ($F = 31.563$, p -value $< .01$) with $Q_{10\text{mg}}$ and $Q_{10\text{m}}$ calculated to be 3.06 ± 0.15 and 1.93 ± 0.14 ($t = 5.571$, p -value $< .01$), respectively. This difference was confirmed for all the sampled years.

ES_{15} was also affected by the different conditions of the monitoring years ($F = 7.094$, p -value = .01) with mean values in 2016 ($0.63 \pm 0.07 \mu\text{mol CO}_2 \text{ m}^{-2} \text{ s}^{-1}$) lower than in 2015 ($0.93 \pm 0.12 \mu\text{mol CO}_2 \text{ m}^{-2} \text{ s}^{-1}$) and 2017 ($0.82 \pm 0.12 \mu\text{mol CO}_2 \text{ m}^{-2} \text{ s}^{-1}$). Similar to Q_{10} , the wood formation period also affected ES_{15} , with $ES_{15\text{mg}}$ ($0.84 \pm 0.22 \mu\text{mol CO}_2 \text{ m}^{-2} \text{ s}^{-1}$) higher than $ES_{15\text{m}}$ ($0.73 \pm 0.02 \mu\text{mol CO}_2 \text{ m}^{-2} \text{ s}^{-1}$, $F = 7.094$, p -value = .01). Furthermore, during the wood formation period, $ES_{15\text{w}}$ was higher in 2015 ($1.03 \pm 0.07 \mu\text{mol CO}_2 \text{ m}^{-2} \text{ s}^{-1}$) and 2017 ($0.90 \pm 0.07 \mu\text{mol CO}_2 \text{ m}^{-2} \text{ s}^{-1}$) than in 2016 ($0.60 \pm 0.09 \mu\text{mol CO}_2 \text{ m}^{-2} \text{ s}^{-1}$). No differences among years were found for ES during the non-wood formation periods.

3.4 | Radial growth and stem CO_2 effluxes

During the study period, annual average measured ES and TRWs were closely related (Figure 8). Seasonal patterns of ES were similar in the 3 years, but with different amplitudes (Figure 9). Moreover, ES_{m} , the stem CO_2 effluxes affected by maintenance respiration, showed a similar pattern among the 3 years. We observed a time-lag between the time of maximum growth rate (t_x) and maximum ES values of 23 ± 2 days, 31 ± 2 days and 29 ± 1 days in 2015, 2016 and 2017, respectively. Differences between years were not significant ($F = 3.317$, p -value = .07).

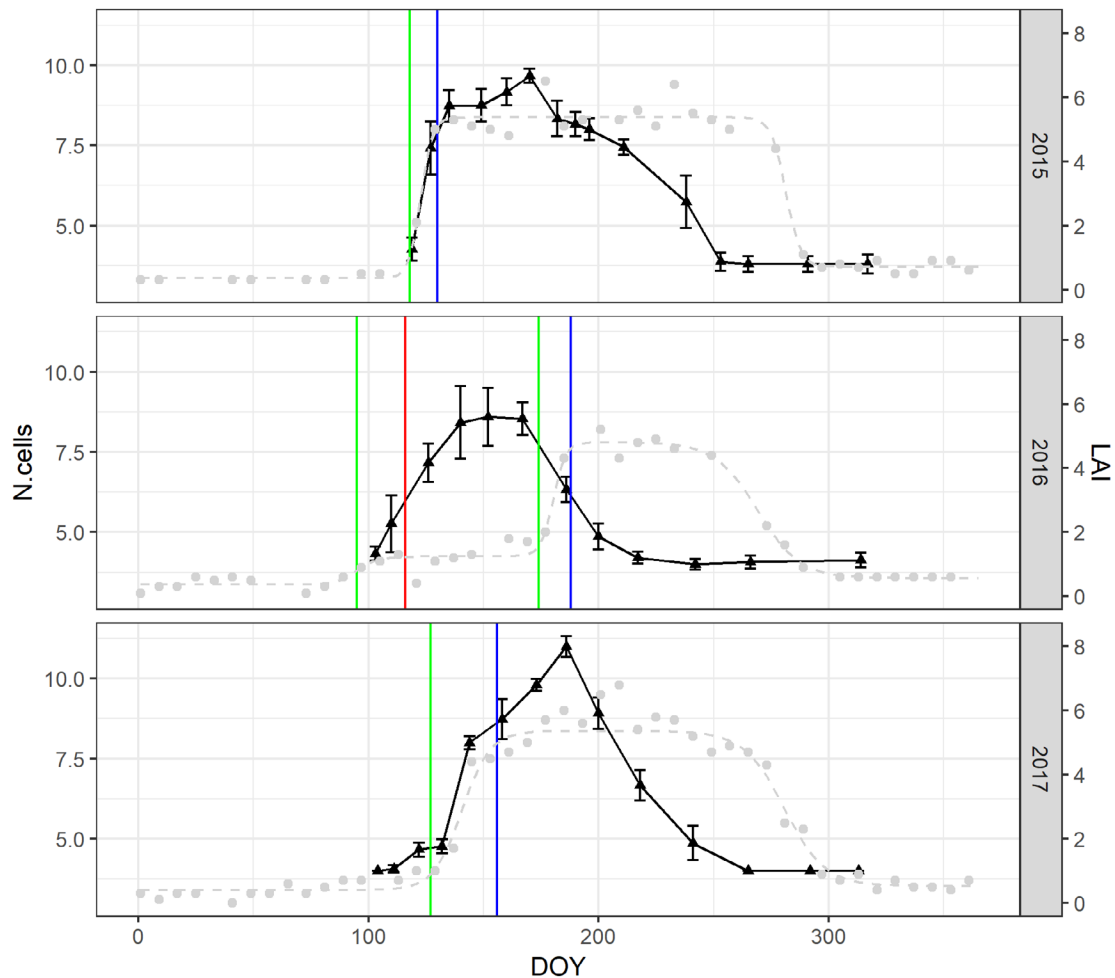


FIGURE 4 Annual trends of the number of cambium cells (N. cells, left Y axis) and leaf area index (LAI, m²/m², right y-axis). Grey circles and dashed lines are the MODIS-LAI values and the modelled intra-annual dynamic at Selva Piana beech forest, respectively. Green and blue vertical lines represent the green-up and maturity phases of leaf phenology, respectively. The red vertical line represents the late frost of April 25, 2016. Black triangles are the average number of cambial cells of the five sampled beech trees. Bars represent ± 1 SE [Colour figure can be viewed at wileyonlinelibrary.com]

3.5 | From single tree to stand level

Annual stand-level stem C emissions (AES_{mg}) were lower in 2016 (0.94 ± 0.11 Mg C ha⁻¹ year⁻¹) than in 2015 (1.34 ± 0.11 Mg C ha⁻¹ year⁻¹) and 2017 (1.23 ± 0.15 Mg C ha⁻¹ year⁻¹) (Table 3). Annual stem C effluxes due to maintenance respiration (AES_m) in 2016 (0.87 ± 0.10 Mg C ha⁻¹ year⁻¹) were lower than in 2015 (1.09 ± 0.07 Mg C ha⁻¹ year⁻¹) and 2017 (1.03 ± 0.12 Mg C ha⁻¹ year⁻¹); AES due to growth respiration (AES_g) was lower in 2016 (0.07 ± 0.02 Mg C ha⁻¹ year⁻¹) than in 2015 (0.24 ± 0.05 Mg C ha⁻¹ year⁻¹) and 2017 (0.20 ± 0.04 Mg C ha⁻¹ year⁻¹). The contribution of AES_g to the annual stem effluxes was 19 ± 0.02 , 7 ± 0.02 and $16 \pm 0.02\%$ in 2015, 2016 and 2017, respectively.

The amount of carbon fixed in the stem biomass (SG) was lower in 2016 (0.28 ± 0.07 Mg C ha⁻¹ year⁻¹) than in 2015 (1.65 ± 0.20 Mg C ha⁻¹ year⁻¹) and 2017 (1.49 ± 0.28 Mg C ha⁻¹ year⁻¹). At the studied beech forest, the mean C construction cost of wood, defined as the slope of the relationship between AES_g and SG at tree level

($R^2 = .842$, p -value $< .01$, see Supporting Information Figure S4), was 0.23 g C emitted per g C fixed. On an annual scale, this parameter was 0.15 ± 0.01 for 2015, 0.24 ± 0.05 for 2016 and 0.14 ± 0.02 for 2017 ($F = 2.797$, p -value = .104).

4 | DISCUSSION

4.1 | Cambial activity and radial growth are not entirely linked to leaf phenology

In all 3 years, cambium reactivation and wood formation occurred within 1–3 weeks after leaf development, confirming the tight dependence of radial growth on leaf phenology and photosynthesis in diffuse-porous species (Čufar et al., 2008; Michelot et al., 2012). Nevertheless, in diffuse-porous trees, stem conductivity to water occurs in several outermost growth rings and is not limited to the youngest formed xylem, as found in ring-porous species (Schume, Grabner, &

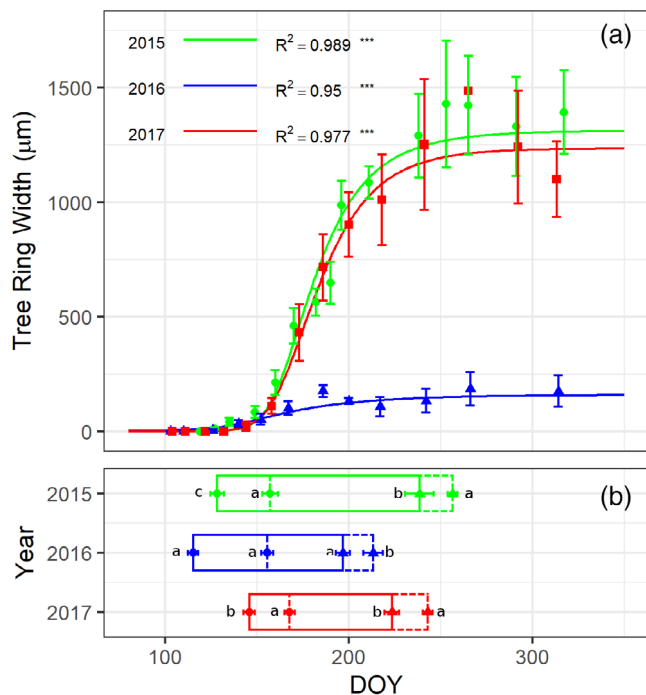


FIGURE 5 Formation and phenology of the xylem. (a) Intra-annual dynamics of xylem formation (μm) in 2015 (green dots and solid line), 2016 (blue dots and solid line) and 2017 (red dots and solid line). Gompertz functions were fitted to the total xylem increment comprised of enlarging, wall thickening and mature cells. Each point is the mean of five sampled *Fagus sylvatica* trees and bars are ± 1 SE, *** p -value $< .001$. (b) Critical dates and duration of wood formation phases. Different letters represent significant differences among the beginning (dots) of the enlargement and the wall thickening phases, cessation (triangle) of the enlargement and the wall thickening phases (p -value $< .05$). Solid and dashed rectangles represent the overall duration of the enlargement and wall thickening phases. Each value is the mean of five sampled trees per year and the bars error represent ± 1 SE [Colour figure can be viewed at wileyonlinelibrary.com]

Eckmüller, 2004). Hence, in beech allocation to the current year wood, it is not as decisive as in ring-porous species, and newly formed photosynthates at the beginning of the season are preferably used for other crucial processes, such as foliage and fine root growth. At the same site, Matteucci (1998) analysed in parallel net ecosystem exchange and carbon allocation to foliage and stem radial growth, finding that the latter started approximately 15 days after photosynthesis exceeded respiration. Until then, net absorbed carbon was allocated mostly to foliage growth. This can be related to the C allocation hierarchy across different C pools, which identifies newly developing leaves as the main C sink at the beginning of the growing season (Capioli et al., 2013; Collalti et al., 2016; Marconi, Chiti, Nolè, Valentini, & Collalti, 2017; Merganičová et al., 2019). Interestingly, and even counter to our expectations, in 2016, the cambium remained active at low rates even after complete canopy defoliation, probably fuelled by old C reserves.

After the re-sprouting of leaves in 2016, cambium cell production decreased and became non-productive, although the environmental

TABLE 2 Parameters describing the intra annual radial growth derived from the Gompertz function for the total xylem increment comprised of enlarging, wall thickening and mature cells

Total xylem increment				
Parameter	Year	Mean (\pm SE)	F	p-Value
α	2015	1,312 (\pm 196) a		
α	2016	230 (\pm 31) b	13.722	$< .01$
α	2017	1,235 (\pm 269) a		
rx	2015	26 (\pm 3) a		
rx	2016	6 (\pm 2) b	8.469	.014
rx	2017	23 (\pm 4) a		
tx	2015	174 (\pm 2) a		
tx	2016	157 (\pm 6) b	22.667	$< .001$
tx	2017	175 (\pm 1) a		

Note: α (μm) is the upper asymptote, representing the final ring width at the end of the growing season; tx (DOY) is the day of the year at which the daily increment is maximum (Gompertz curve inflection point); rx is the maximum daily increment ($\mu\text{m day}^{-1}$). Different letters represent significant differences among the monitored years.

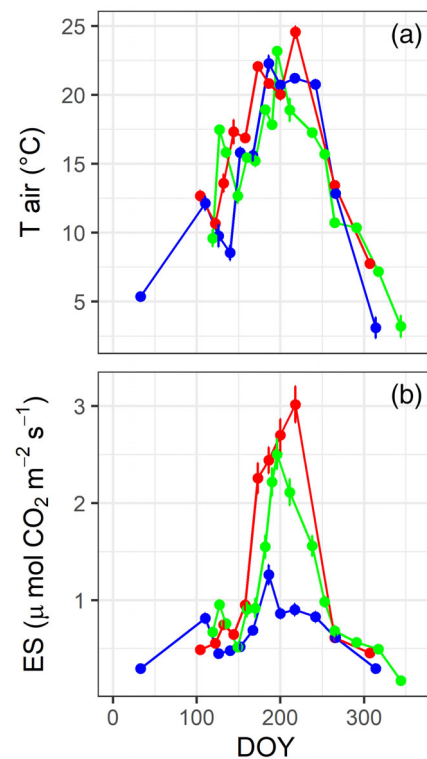


FIGURE 6 (a) T_{air} ($^{\circ}\text{C}$) at the day of sampling in 2015 (green), 2016 (blue) and 2017 (red). (b) Measured stem CO_2 effluxes ($\mu\text{mol CO}_2 \text{m}^{-2} \text{s}^{-1}$) in 2015 (green), 2016 (blue) and 2017 (red). Each point is the mean of five *Fagus sylvatica* trees. Bars are ± 1 SE [Colour figure can be viewed at wileyonlinelibrary.com]

conditions were potentially still favourable for radial growth (Camarero, Olano, & Parras, 2010; Rossi et al., 2006). Stem radial growth of beech in Selva Piana was greatly affected by the extreme

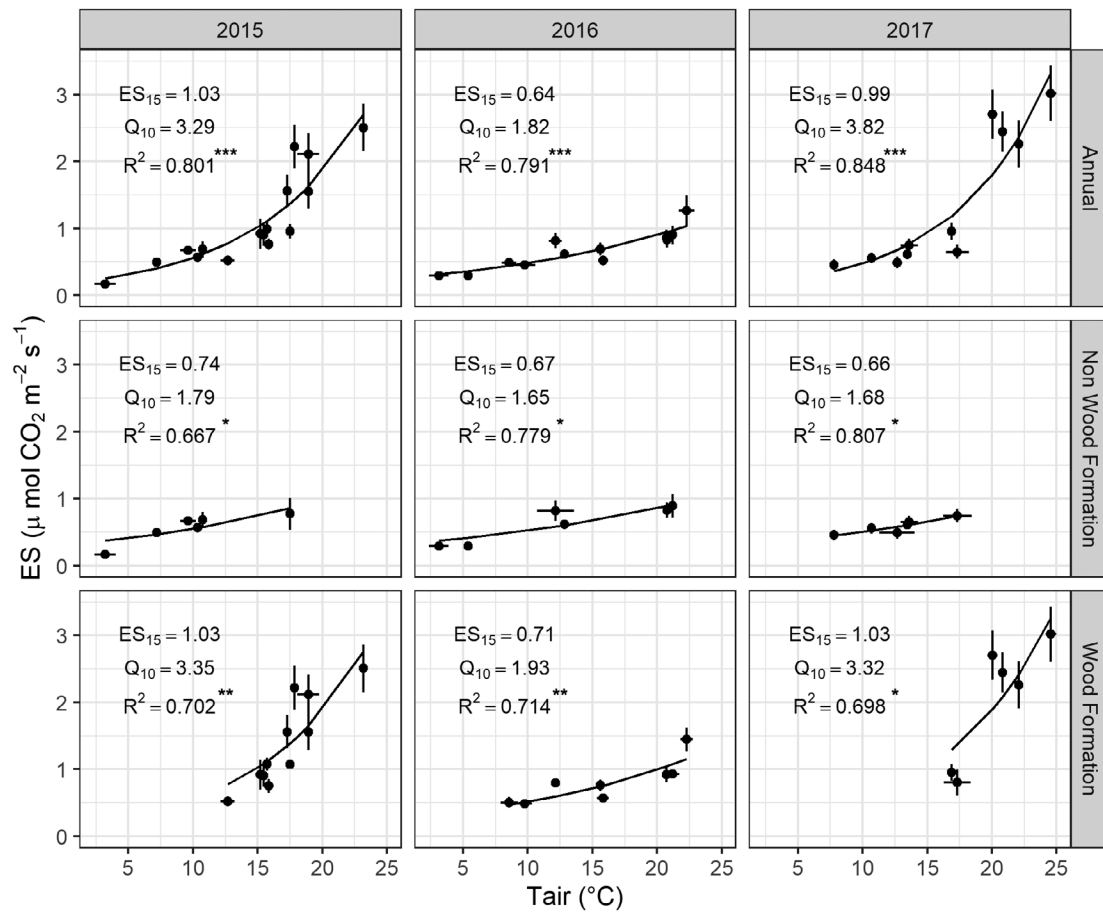


FIGURE 7 Relationship between ES ($\mu\text{mol CO}_2 \text{ m}^{-2} \text{ s}^{-1}$) and air temperature (T_{air} , °C). Annual, considering the whole measurements for each year, each point is the mean of five sampled trees. Each point represents the mean of those trees, which are in the non-wood and wood formation periods, at a given sampling date. Bars are ± 1 SE. *** p -Value $< .001$, ** p -value $< .01$, * p -value $< .05$

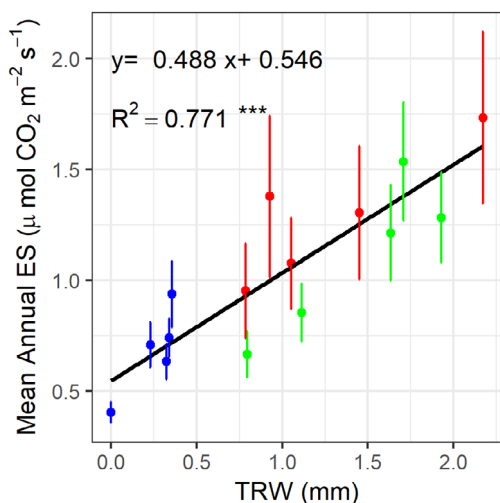


FIGURE 8 Relationships between ring widths (mm) and the mean annual ES ($\mu\text{mol CO}_2 \text{ m}^{-2} \text{ s}^{-1}$) measured in 2015 (green), 2016 (blue) and 2017 (red). Each point represents a sampled *Fagus sylvatica* tree per year. Bars represent ± 1 SE. *** p -value $< .001$ [Colour figure can be viewed at wileyonlinelibrary.com]

late spring frost in 2016 because of the premature cessation of cambial cell production and the lower growth rate during the active period, which resulted in 82% narrower annual xylem increments compared to 2015 and 2017. Hence, after this stressful event, trees preferred to prioritize C resources allocation to newly developing leaves and to reserve C pools, the new main C sinks, rather than radial growth. In beech, previously reported growth reduction—as a consequence of late frost—ranged from 48 to 83%, with the maximum occurring at the northern fringe of the Alps (Dittmar et al., 2006). At the studied stand, radial growth rates had fully recovered in 2017, with no visible long-term effects of the late spring frost event in 2016, showing the high resilience of beech growth to late frost (Dittmar et al., 2006; Principe, Struwe, Wilmking, & Kreyling, 2017). However, as recently shown in D'Andrea et al. (2019), beech trees during 2016 were able to compensate the lost C reserve, completely refilling the pool to the same level as before the frost event. Hence, there was no need to prioritize reserve recharge over stem biomass production the subsequent year.

The 2017 summer drought became severe only in August (SPEI < 1.5), when the trees had already completed most of their

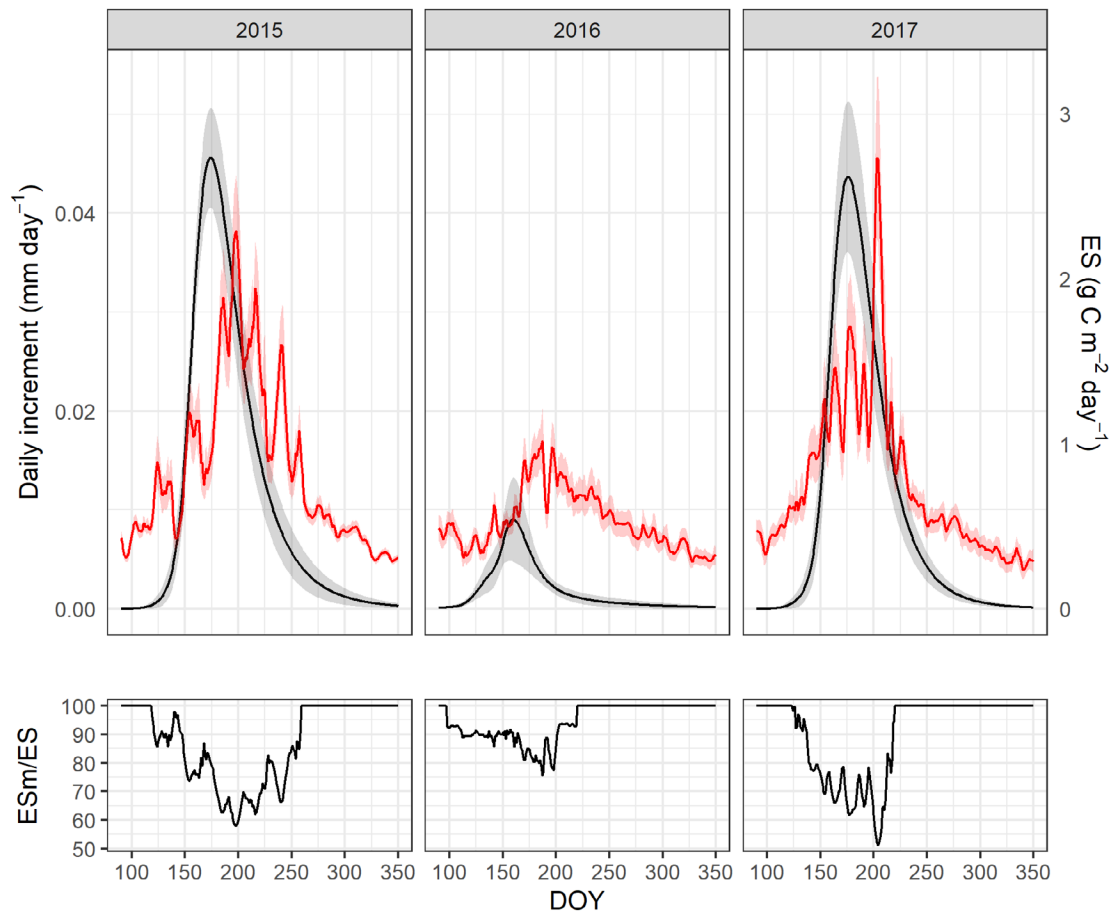


FIGURE 9 Daily stem increment and stem carbon effluxes of *Fagus sylvatica* at stand level. Top panel: the black line is the daily increment during 2015, 2016 and 2017, respectively. The red line represents ES, the daily C effluxes. Lower panel: contribution of maintenance respiration to daily stem CO₂ efflux calculated as ES_m/ES_{mg} [Colour figure can be viewed at wileyonlinelibrary.com]

TABLE 3 Annual C stem fluxes

Year	Flux type	Mean \pm SE Mg C ha ⁻¹ year ⁻¹	F	p-Value
2015	AESgm	1.34 \pm 0.12 a		
2016	AESgm	0.94 \pm 0.11b	13.808	.003
2017	AESgm	1.23 \pm 0.15a		
2015	AESm	1.09 \pm 0.07a		
2016	AESm	0.87 \pm 0.10 b	8.015	.012
2017	AESm	1.03 \pm 0.12 a		
2015	AESg	0.24 \pm 0.05 a		
2016	AESg	0.07 \pm 0.05 b	7.634	.014
2017	AESg	0.20 \pm 0.04 a		
2015	SG	1.65 \pm 0.20 a		
2016	SG	0.28 \pm 0.07 b	18.639	.001
2017	SG	1.49 \pm 0.28 a		

Note: AESgm is the annual stem C efflux assessed using specific parameters for wood formation (Q_{10w} and ES_{15w}) and non-wood formation phases (Q_{10nw} and ES_{15nw}); AESm is the annual stem C efflux due to maintenance respiration; AESg is the annual stem C efflux due to growth respiration; SG is the annual amount of C fixed in the stem biomass; different letters represent significant differences p value $< .05$.

radial growth, as already seen for other tree species growing in the Mediterranean adjusting the end xylem growth before potential stressful conditions may occur (e.g., Forner, Valladares, Bonal, Granier, & Grossiord, 2018; Lempereur et al., 2015). Instead, the importance of favourable spring climatic conditions on beech growth has been reported for the Apennines and the Eastern Alps (Di Filippo, Biondi, Maugeri, Schirone, & Piovesan, 2012; Piovesan, Biondi, di Filippo, Alessandrini, & Maugeri, 2008).

4.2 | Effluxes from stem are not entirely synchronised to radial growth

Our results, being measured ES lower in 2016 despite similar air temperatures during the three monitoring years, demonstrated that stem CO₂ efflux cannot uniquely be estimated from temperature data. Mean annual values of “apparent” Q₁₀ ranged between 2.11 (2016) and 2.71 (2015) and were similar to the values estimated at the same site for co-dominant (2.59) and dominant (2.34) trees described in Guidolotti et al., 2013. Q_{10m} and Q_{10mg} estimated in this study are closely comparable with the dataset of various coniferous and broad-leaf tree species as reported in Damesin et al. (2002). Similar intra-annual variability of Q₁₀ has also been observed in many other studies for different tree species, with higher Q₁₀ during the growing period (Carey et al., 1997; Gruber et al., 2009; Paembonan, Hagihara, & Hozumi, 1992; Stockfors & Linder, 1998). A higher Q₁₀ during the wood formation period compared to the non-wood formation period can be explained by including the “apparent” growth respiration in the parameters' estimates. This only “apparent” increase of Q₁₀ is driven by the indirect effect of temperature on stem growth, which adds up to the maintenance respiration sensitivity to temperature (Salomón, de Schepper, Valbuena-Carabaña, Gil, & Steppe, 2018). However, other studies found (or assume) stable Q₁₀ throughout the year (see, e.g., Ceschia et al., 2002; Damesin et al., 2002). Similarly, the analysis of 136 Q₁₀ values from stem respiration showed a mean value of 2.18, with 42% of the values in the range from 1.5 to 2.0 and (Wang, Wang, Zu, Li, & Takayoshi, 2006).

As reported in other studies, the stem CO₂ efflux at an air temperature of 15°C, ES₁₅, was sensitive to wood formation processes, showing an increase during the growing period (Ceschia et al., 2002; Damesin et al., 2002).

Maximum xylem production and maximum ES were not synchronized and an almost constant delay, of about 1 month, was observed, as similarly found in a young beech forest in which peak ES occurred about 27 days after the maximum stem growth rate (Ceschia et al., 2002). Similarly, in an Australian stand dominated by *Eucalyptus tereticornis* Sm. a time-lag of 43 days was also observed (Salomón, Steppe, Crous, Noh, & Ellsworth, 2019). Furthermore, our results confirmed that the peak of ES occurred when xylem cells were still in the phase of wall thickening and lignification, as previously hypothesized (Ceschia et al., 2002). Moreover, when maximum ES was observed, it is very likely that trees were already refilling the stem C reserves pool (Scartazza, Moscatello, Matteucci, Battistelli, & Brugnoli, 2013).

4.3 | Only spring frost affects negatively stem C fluxes

The amount of C fixed by stem biomass formation in 2015 and 2017 were 1.65 and 1.49 Mg C ha⁻¹ year⁻¹, lower than the values reported for a beech forest growing in plain in Germany that ranged between 1.69 and 2.41 Mg C ha⁻¹ year⁻¹ (Mund et al., 2010). In 2016, however, we measured only 0.28 ± 0.07 Mg C ha⁻¹ year⁻¹, that is, only about 20% of the fixation during the two other years, emphasizing how exceptionally negative this year was.

Annual stem CO₂ efflux (AES) is known to be highly variable in temperate forests (Yang et al., 2016). Our data range from 0.94 to 1.34 Mg C ha⁻¹ year⁻¹ and thus is lower than 1.65 to 2.25 Mg C ha⁻¹ year⁻¹ reported for a younger beech forest (Damesin et al., 2002). An earlier estimate of AES at the study site was 0.63 Mg C ha⁻¹ year⁻¹ (Guidolotti et al., 2013) for 2007, year characterized by an extreme summer drought (SPEI < -2). The stem C efflux of the drought year presented in this study (2017, 1.23 Mg C ha⁻¹ year⁻¹) was about the double than 2007, which could be due to an increase in stem biomass (ca. 15% lower in 2007 than in 2017), to different measurement tools and to the stronger drought. The contribution of AES_g to annual stem effluxes, ranging from 7 to 19%, was lower than that measured in a young beech forest (Ceschia et al., 2002), evidencing the importance of forest developmental stage in determining wood formation, growth respiration and their role in stand carbon balance.

The construction cost we found of 0.23 g C emitted per g C fixed is consistent with the lower range of values reported for beech from 0.2 to 0.4 g C fixed per g C emitted (Ceschia et al., 2002; Damesin et al., 2002). A large range of construction cost, from 0.16 to 0.87 g C emitted per g C fixed, were reported in Rodríguez-Calcerrada et al. (2019). The dataset includes different method for estimating construction costs, and their variability underlines how analytical methods affect the estimation of the respiratory component (Rodríguez-Calcerrada et al., 2019).

The late frost event in 2016 reduced both wood growth and stem CO₂ efflux with respect to those measured in the other 2 years, but the percentage of growth reduction (80%) was much larger than the reduction of ES (25%). In this year, the strong reduction of fixed C, and the contemporary lower reduction of stem CO₂ efflux, strongly affected the overall stem carbon balance. Results suggest that maintenance metabolism and respiration is mandatory for tree survival, even tapping on different C source (e.g., old C reserves). Moreover, the ability of modifying the sink hierarchy, reducing allocation to radial growth, allowed trees to face such stressful event. In contrast, the summer drought in 2017 did not have any effect on stem growth, and thus neither on CO₂ efflux due to growth respiration. Indeed, the summer drought became severe only in August when beech trees already completed the enlargement phase and most of the wall thickening/lignification, and ultimately, causing a negligible reduction of associated respiratory cost.

In conclusion, this study further highlights the sensitivity of European beech to leaf damage due to late spring frost. Since leaf development is expected to start earlier for beeches (and not only)

due to global warming, the likelihood that spring frost may damage leaves will increase, as it is already occurring in Europe. We demonstrated that stem growth was significantly reduced due to the prolonged absence of photosynthesizing leaves after frost, since beech trees tapped their pool of old C reserves. However, the loss in growth was not completely compensated for after re-growth of leaves, but rather the cambium activity ceased shortly thereafter. Consequently, the trees fixed less C in the stem biomass, showing also a reduction of the stem carbon efflux related to growth respiration. Moreover, the summer drought occurred too late to affect wood formation and stem CO₂ effluxes. However, more investigations are needed to evaluate its effects on other physiological processes. This study also underlines the crucial role of spring weather conditions on the growth and physiology of beech trees. A better understanding of fine scale C dynamic will help in evaluating a medium- to long-term response to climate change under an increasing frequency of extreme events.

ACKNOWLEDGMENTS

The activities of Negar Rezaie at the wood anatomy laboratory of Slovenian Forestry Institute were supported by an Excellence Research Award of the National Research Council of Italy, Department of Biology, Agriculture, and Food Secures (Prot. 71951, 06/11/2017). Collelongo-Selva Piana is one of the sites of the Italian Long-Term Ecological Research network (LTER-Italy), part of the International LTER network (ILTER). Research at the site in the years of this study was funded by the eLTER H2020 Project (grant agreement no. 654359). Activity and data analysis at the site is currently funded by resources available from the Italian Ministry of University and Research (FOE-2019), under projects Climate Changes (CNR DTA AD003.474) and Green & Circular Economy—GECE (CNR DBA AD003.139). The authors are grateful to Martin Cregeen for English language editing. The authors also are grateful to the anonymous reviewers and subject Editor for their constructive comments to improve the manuscript in a spirit of full collaboration.

CONFLICT OF INTEREST

The authors declare no potential sources of conflict of interest.

ORCID

Ettore D'Andrea  <https://orcid.org/0000-0002-5884-210X>

Negar Rezaie  <https://orcid.org/0000-0002-8487-2345>

Peter Prislán  <https://orcid.org/0000-0002-3932-6388>

Jozica Gričar  <https://orcid.org/0000-0001-5207-1466>

Alessio Collalti  <https://orcid.org/0000-0002-4980-8487>

Jan Muhr  <https://orcid.org/0000-0001-5264-0243>

Giorgio Matteucci  <https://orcid.org/0000-0002-4790-9540>

REFERENCES

- Allevato, E., Saulino, L., Cesarano, G., Chirico, G. B., D'Urso, G., Falanga Bolognesi, S., ... Bonanomi, G. (2019). Canopy damage by spring frost in European beech along the Apennines: Effect of latitude, altitude and aspect. *Remote Sensing of Environment*, 225, 431–440.
- Amthor, J. S. (2000). The McCree - de Wit - Penning de Vries - Thornley respiration paradigms: 30 years later. *Annals of Botany*, 86, 1–20.
- Augsburger, C. K. (2013). Reconstructing patterns of temperature, phenology, and frost damage over 124 years: Spring damage risk is increasing. *Ecology*, 94, 41–50.
- Bascietto, M., Bajocco, S., Mazzenga, F., & Matteucci, G. (2018). Assessing spring frost effects on beech forests in central Apennines from remotely-sensed data. *Agricultural and Forest Meteorology*, 248, 240–250.
- Bascietto, M., Cherubini, P., & Scarascia-Mugnozza, G. (2004). Tree rings from a European beech forest chronosequence are useful for detecting growth trends and carbon sequestration. *Canadian Journal of Forest Research*, 34, 481–492.
- Begum, S., Nakaba, S., Oribe, Y., Kubo, T., & Funada, R. (2007). Induction of cambial reactivation by localized heating in a deciduous hardwood hybrid poplar (*Populus sieboldii* 3 P. grandidentata). *Annals of Botany*, 100, 439–447.
- Bloemen, J., Agneessens, L., van Meulebroek, L., Aubrey, D. P., McGuire, M. A., Teskey, R. O., & Steppe, K. (2014). Stem girdling affects the quantity of CO₂ transported in xylem as well as CO₂ efflux from soil. *New Phytologist*, 201, 897–907.
- Bloemen, J., McGuire, M. A., Aubrey, D. P., Teskey, R. O., & Steppe, K. (2013). Transport of root-respired CO₂ via the transpiration stream affects aboveground carbon assimilation and CO₂ efflux in trees. *New Phytologist*, 197, 555–565.
- Bowman, W. P., Barbour, M. M., Turnbull, M. H., Tissue, D. T., Whitehead, D., & Griffin, K. L. (2005). Sap flow rates and sapwood density are critical factors in within- and between-tree variation in CO₂ efflux from stems of mature *Dacrydium cupressinum* trees. *New Phytologist*, 167, 815–828.
- Camarero, J. J., Guerrero-Campo, J., & Gutierrez, E. (1998). Tree-ring growth and structure of *Pinus uncinata* and *Pinus sylvestris* in the central Spanish Pyrenees. *Arctic and Alpine Research*, 30(1), 1.
- Camarero, J. J., Olano, J. M., & Parras, A. (2010). Plastic bimodal xylogenesis in conifers from continental Mediterranean climates. *New Phytologist*, 185, 471–480.
- Campiolli, M., Verbeeck, H., van den Bossche, J., Wu, J., Ibrom, A., D'Andrea, E., ... Granier, A. (2013). Can decision rules simulate carbon allocation for years with contrasting and extreme weather conditions? A case study for three temperate beech forests. *Ecological Modelling*, 263, 42–55.
- Carey, E. V., Callaway, R. M., & DeLucia, E. H. (1997). Stem respiration of ponderosa pines grown in contrasting climates: Implications for global climate change. *Oecologia*, 111, 19–25.
- Carrer, M., Brunetti, M., & Castagneri, D. (2016). The imprint of extreme climate events in century-long time series of wood anatomical traits in high-elevation conifers. *Frontiers in Plant Science*, 7, 1–12.
- Ceschia, É., Damesin, C., Lebaube, S., Pontailleur, J. Y., & Dufréne, É. (2002). Spatial and seasonal variations in stem respiration of beech trees (*Fagus sylvatica*). *Annals of Forest Science*, 59, 801–812.
- Chan, T., Berninger, F., Kolari, P., Nikinmaa, E., & Hölttä, T. (2018). Linking stem growth respiration to the seasonal course of stem growth and GPP of scots pine. *Tree Physiology*, 38, 1356–1370.
- Collalti, A., Marconi, S., Ibrom, A., Trotta, C., Anav, A., D'Andrea, E., ... Santini, M. (2016). Validation of 3D-CMCC forest ecosystem model (v. 5. 1) against eddy covariance data for 10 European forest sites. *Geoscientific Model Development*, 9, 479–504.
- Collalti, A., Tjoelker, M. G., Hoch, G., Mäkelä, A., Guidolotti, G., Heskell, M., ... Prentice, I. C. (2020). Plant respiration: Controlled by photosynthesis or biomass? *Global Change Biology*, 26, 1739–1753.
- Collalti, A., Trotta, C., Keenan, T. F., Ibrom, A., Bond-lamberty, B., Grote, R., ... Reyer, C. P. O. (2018). Thinning can reduce losses in carbon use efficiency and carbon stocks in managed forests under warmer climate. *Journal of Advances in Modeling Earth Systems*, 10, 2427–2452.

- Čufar, K., Prislán, P., de Luis, M., & Gričar, J. (2008). Tree-ring variation, wood formation and phenology of beech (*Fagus sylvatica*) from a representative site in Slovenia, SE Central Europe. *Trees - Structure and Function*, 22, 749–758.
- Cuny, H. E., Rathgeber, C. B. K., Frank, D., Fonti, P., Mäkinen, H., Prislán, P., ... Fournier, M. (2015). Woody biomass production lags stem-girth increase by over one month in coniferous forests. *Nature Plants*, 1, 15160.
- Damesin, C., Ceschia, E., le Goff, N., Ottorini, J.-M., & Dufrière, E. (2002). Stem and branch respiration of beech: From tree measurements to estimations at the stand level. *New Phytologist*, 153, 159–172.
- D'Andrea, E., Guidolotti, G., Scartazza, A., De Angelis, P., & Matteucci, G. (2020). Small-scale forest structure influences spatial variability of belowground carbon fluxes in a mature Mediterranean beech forest. *Forests*, 11, 255.
- D'Andrea, E., Rezaie, N., Battistelli, A., Gavrichkova, O., Kuhlmann, I., Matteucci, G., ... Muhr, J. (2019). Winter's bite: Beech trees survive complete defoliation due to spring late-frost damage by mobilizing old C reserves. *New Phytologist*, 224, 625–631.
- Delpierre, N., Lireux, S., Hartig, F., Camarero, J. J., Cheaib, A., Čufar, K., ... Rathgeber, C. B. K. (2019). Chilling and forcing temperatures interact to predict the onset of wood formation in Northern Hemisphere conifers. *Global Change Biology*, 25, 1089–1105.
- DeRoo, L., Salomón, R. L., & Steppe, K. (2020). Woody tissue photosynthesis reduces stem CO₂ efflux by half and remains unaffected by drought stress in young *Populus tremula* trees. *Plant, Cell & Environment*, 43, 981–991.
- Deslauriers, A., Rossi, S., Anfodillo, T., & Saracino, A. (2008). Cambial phenology, wood formation and temperature thresholds in two contrasting years at high altitude in southern Italy. *Tree Physiology*, 28, 863–871.
- Di Filippo, A., Biondi, F., Maugeri, M., Schirone, B., & Piovesan, G. (2012). Bioclimate and growth history affect beech lifespan in the Italian Alps and Apennines. *Global Change Biology*, 18, 960–972.
- Dittmar, C., Fricke, W., & Elling, W. (2006). Impact of late frost events on radial growth of common beech (*Fagus sylvatica* L.) in Southern Germany. *European Journal of Forest Research*, 125, 249–259.
- Forner, A., Valladares, F., Bonal, D., Granier, A., & Grossiord, C. (2018). Extreme droughts affecting Mediterranean tree species' growth and water-use efficiency: The importance of timing. *Tree Physiology*, 38, 1127–1137.
- Frank, D., Reichstein, M., Bahn, M., Thonicke, K., Frank, D., Mahecha, M. D., ... Zscheischler, J. (2015). Effects of climate extremes on the terrestrial carbon cycle: Concepts, processes and potential future impacts. *Global Change Biology*, 21, 2861–2880.
- Gazol, A., Camarero, J. J., Colangelo, M., de Luis, M., Martínez del Castillo, E., & Serra-Maluquer, X. (2019). Summer drought and spring frost, but not their interaction, constrain European beech and silver fir growth in their southern distribution limits. *Agricultural and Forest Meteorology*, 278, 107695.
- Gordo, O., & Sanz, J. J. (2010). Impact of climate change on plant phenology in Mediterranean ecosystems. *Global Change Biology*, 16, 1082–1106.
- Greco, S., Infusino, M., de Donato, C., Coluzzi, R., Imbrenda, V., Lanfredi, M., ... Scalerio, S. (2018). Late spring frost in Mediterranean beech forests: Extended crown dieback and short-term effects on moth communities. *Forests*, 9, 1–18.
- Gričar, J., Krže, L., & Čufar, K. (2009). Number of cells in xylem, phloem and dormant cambium in silver fir (*Abies alba*), in trees of different vitality. *IAWA Journal*, 30, 121–133.
- Gruber, A., Wieser, G., & Oberhuber, W. (2009). Intra-annual dynamics of stem CO₂ efflux in relation to cambial activity and xylem development in *Pinus cembra*. *Tree Physiology*, 29, 641–649.
- Guidolotti, G., Rey, A., D'Andrea, E., Matteucci, G., & de Angelis, P. (2013). Effect of environmental variables and stand structure on ecosystem respiration components in a Mediterranean beech forest. *Tree Physiology*, 33, 960–972.
- Hilman, B., Muhr, J., Trumbore, S. E., Kunert, N., Carbone, M. S., Yuval, P., ... Angert, A. (2019). Comparison of CO₂ and O₂ fluxes demonstrate retention of respired CO₂ in tree stems from a range of tree species. *Biogeosciences*, 16, 177–191.
- Katayama, A., Kume, T., Ichihashi, R., & Nakagawa, M. (2019). Vertical variation in wood CO₂ efflux is not uniformly related to height: Measurement across various species and sizes of Bornean tropical rainforest trees. *Tree Physiology*, 39, 1000–1008.
- Lempereur, M., Martin-stpaul, N. K., Damesin, C., Joffre, R., Ourcival, J., Rocheteau, A., & Rambal, S. (2015). Growth duration is a better predictor of stem increment than carbon supply in a Mediterranean oak forest: implications for assessing forest productivity under climate change. *New Phytologist*, 207, 579–590.
- Linares, J. C., Camarero, J. J., & Carreira, J. A. (2009). Plastic responses of *Abies pinsapo* xylogenesis to drought and competition. *Tree Physiology*, 29, 1525–1536.
- Marconi, S., Chiti, T., Nolè, A., Valentini, R., & Collalti, A. (2017). The role of respiration in estimation of net carbon cycle: Coupling soil carbon dynamics and canopy turnover in a novel version of 3D-CMCC forest ecosystem model. *Forests*, 8, 220.
- Masci, A. (2002). Biomassa, produttività primaria netta e mineralomassa in una faggeta dell'Appennino centrale.
- Matteucci, G. (1998). *Bilancio del carbonio in una faggeta dell'Italia Centro-Meridionale: Determinanti ecofisiologici, integrazione a livello di copertura e simulazione dell'impatto dei cambiamenti ambientali*. Padova, Italy: Università degli studi di Padova.
- Meir, P., Mencuccini, M., & Coughlin, S. I. (2019). Respiration in wood: Integrating across tissues, functions and scales. *New Phytologist*, 225, 1824–1827.
- Merganičová, K., Merganič, J., Lehtonen, A., Vacchiano, G., Sever, M. Z. O., Augustynczyk, A. L. D., ... Reyer, C. P. O. (2019). Forest carbon allocation modelling under climate change. *Tree Physiology*, 39, 1937–1960.
- Michelot, A., Simard, S., Rathgeber, C., Dufrière, E., & Damesin, C. (2012). Comparing the intra-annual wood formation of three European species (*Fagus sylvatica*, *Quercus petraea* and *Pinus sylvestris*) as related to leaf phenology and non-structural carbohydrate dynamics. *Tree Physiology*, 32, 1033–1045.
- Mund, M., Kutsch, W. L., Wirth, C., Kahl, T., Knohl, A., Skomarkova, M. V., & Schulze, E.-D. (2010). The influence of climate and fructification on the inter-annual variability of stem growth and net primary productivity in an old-growth, mixed beech forest. *Tree Physiology*, 30, 689–704.
- Nolè, A., Rita, A., Ferrara, A. M. S., & Borghetti, M. (2018). Effects of a large-scale late spring frost on a beech (*Fagus sylvatica* L.) dominated Mediterranean mountain forest derived from the spatio-temporal variations of NDVI. *Annals of Forest Science*, 75, 83.
- Oladi, R., Pourtahmasi, K., Eckstein, D., & Bräuning, A. (2011). Seasonal dynamics of wood formation in oriental beech (*Fagus orientalis* Lipsky) along an altitudinal gradient in the Hyrcanian forest, Iran. *Trees - Structure and Function*, 25, 425–433.
- Paembonan, S. A., Hagiwara, A., & Hozumi, K. (1992). Long-term respiration in relation to growth and maintenance processes of the above-ground parts of a hinoki forest tree. *Tree Physiology*, 10, 21–31.
- Pastorello, G., Trotta, C., Canfora, E., Chu, H., Christianson, D., Cheah, Y.-W., ... Papale, D. (2020). The FLUXNET2015 dataset and the ONEFlux processing pipeline for eddy covariance data. *Scientific Data*, 7, 225.
- Peuke, A. D., Schraml, C., Hartung, W., & Rennenberg, H. (2002). Identification of drought-sensitive beech ecotypes by physiological parameters. *New Phytologist*, 154, 373–387.
- Piovesan, G., Biondi, F., di Filippo, A., Alessandrini, A., & Maugeri, M. (2008). Drought-driven growth reduction in old beech (*Fagus sylvatica* L.) forests of the central Apennines, Italy. *Global Change Biology*, 14, 1265–1281.

- Principe, A., Struwe, T., Wilmking, M., & Kreyling, J. (2017). Low resistance but high resilience in growth of a major deciduous forest tree (*Fagus sylvatica* L.) in response to late spring frost in southern Germany. *Trees - Structure and Function*, 31, 743–751.
- Prislan, P., Čufar, K., De Luis, M., & Gričar, J. (2018). Precipitation is not limiting for xylem formation dynamics and vessel development in European beech from two temperate forest sites. *Tree Physiology*, 38, 186–197.
- Prislan, P., Gričar, J., de Luis, M., Smith, K. T., & Cufar, K. (2013). Phenological variation in xylem and phloem formation in *Fagus sylvatica* from two contrasting sites. *Agricultural and Forest Meteorology*, 180, 142–151.
- R Development Core Team. (2018). *R: A language and environment for statistical computing*. Vienna, Austria: R Foundation for Statistical Computing.
- Rathgeber, C. B. K., Rossi, S., & Bontemps, J.-D. (2011). Cambial activity related to tree size in a mature silver-fir plantation. *Annals of Botany*, 108, 429–438.
- Rathgeber, C. B. K., Santenoise, P., & Cuny, H. E. (2018). CAVIAR: An R package for checking, displaying and processing wood-formation-monitoring data. *Tree Physiology*, 38, 1246–1260.
- Reyer, C. P. O., Silveyra Gonzalez, R., Dolos, K., Hartig, F., Hauf, Y., Noack, M., ... Frieler, K. (2020). The PROFOUND database for evaluating vegetation models and simulating climate impacts on European forests. *Earth System Science Data*, 12, 1295–1320.
- Rezaie, N., D'Andrea, E., Bräuning, A., Matteucci, G., Bombi, P., & Lauteri, M. (2018). Do atmospheric CO₂ concentration increase, climate and forest management affect iWUE of common beech? Evidences from carbon isotope analyses in tree rings. *Tree Physiology*, 1975, 1110–1126.
- Rissanen, K., Vanhatalo, A., Salmon, Y., Bäck, J., & Hölttä, T. (2020). Stem emissions of monoterpenes, acetaldehyde and methanol from scots pine (*Pinus sylvestris* L.) affected by tree–water relations and cambial growth. *Plant Cell and Environment*, 43, 1751–1765.
- Rita, A., Camarero, J. J., & Nolè, A. (2020). The impact of drought spells on forests depends on site conditions: The case of 2017 summer heat wave in southern Europe. *Glob Change Biology*, 26, 851–863. <https://doi.org/10.1111/gcb.14825>
- Rodríguez-Calcerrada, J., Salomón, R. L., Gordaliza, G. G., Miranda, J. C., Miranda, E., de la Riva, E. G., & Gil, L. (2019). Respiratory costs of producing and maintaining stem biomass in eight co-occurring tree species. *Tree Physiology*, 39, 1838–1854.
- Rossi, S., Deslauriers, A., Anfodillo, T., Morin, H., Saracino, A., Motta, R., & Borghetti, M. (2006). Conifers in cold environments synchronize maximum growth rate of tree-ring formation with day length. *New Phytologist*, 170, 301–310.
- Rossi, S., Menardi, R., Fontanella, F., & Anfodillo, T. (2005). Campionatore Trephor: Un nuovo strumento per l'analisi della xilogenesi in specie legnose. *Dendronatura*, 1, 60–67.
- Salomón, R. L., de Schepper, V., Valbuena-Carabaña, M., Gil, L., & Steppe, K. (2018). Daytime depression in temperature-normalised stem CO₂ efflux in young poplar trees is dominated by low turgor pressure rather than by internal transport of respired CO₂. *New Phytologist*, 217, 586–598.
- Salomón, R. L., Steppe, K., Crous, K. Y., Noh, N. J., & Ellsworth, D. S. (2019). Elevated CO₂ does not affect stem CO₂ efflux nor stem respiration in a dry eucalyptus woodland, but it shifts the vertical gradient in xylem [CO₂]. *Plant Cell and Environment*, 42, 2151–2164.
- Saveyn, A., Steppe, K., Mc Guire, M. A., Lemeur, R., & Teskey, A. R. O. (2008). Stem respiration and carbon dioxide efflux of young *Populus deltoides* trees in relation to temperature and xylem carbon dioxide concentration. *Oecologia*, 154, 637–649.
- Scarascia-Mugnozza, G., Bauer, G. A., Persson, H., Matteucci, G., & Masci, A. (2000). Tree biomass, growth and nutrient pools. In E.-D. Schulze (Ed.), *Carbon and nitrogen cycling in European forest ecosystems Ecological studies* (pp. 49–62). New York: Springer Verlag.
- Scartazza, A., Moscatello, S., Matteucci, G., Battistelli, A., & Brugnoli, E. (2013). Seasonal and inter-annual dynamics of growth, non-structural carbohydrates and C stable isotopes in a Mediterranean beech forest. *Tree Physiology*, 33, 730–742.
- Schröter, D., Cramer, W., Leemans, R., Prentice, I. C., Araújo, M. B., Arnell, N. W., ... Zierl, B. (2005). Ecosystem service supply and vulnerability to global change in Europe. *Science*, 310, 1333–1337.
- Schume, H., Grabner, M., & Eckmüllner, O. (2004). The influence of an altered groundwater regime on vessel properties of hybrid poplar. *Trees*, 18, 184–194.
- Stockfors, J., & Linder, S. (1998). Effect of nitrogen on the seasonal course of growth and maintenance respiration in stems of Norway spruce trees. *Tree Physiology*, 18, 155–166.
- Teskey, R. O., & McGuire, M. A. (2007). Measurement of stem respiration of sycamore (*Platanus occidentalis* L.) trees involves internal and external fluxes of CO₂ and possible transport of CO₂ from roots. *Plant, Cell and Environment*, 30, 570–579.
- Teskey, R. O., Saveyn, A., Steppe, K., & McGuire, M. A. (2008). Origin, fate and significance of CO₂ in tree stems. *New Phytologist*, 177, 17–32.
- Thornley, J. H. M. (1970). Respiration, growth and maintenance in plants. *Nature*, 227, 304–305.
- Trumbore, S. E., Angert, A., Kunert, N., Muhr, J., & Chambers, J. Q. (2013). What's the flux? Unraveling how CO₂ fluxes from trees reflect underlying physiological processes. *New Phytologist*, 197, 353–355.
- Vicente-Serrano, S. M., Gouveia, C., Camarero, J. J., Begueria, S., Trigo, R., López-Moreno, J. I., ... Sanchez-Lorenzo, A. (2013). Response of vegetation to drought time-scales across global land biomes. *Proceedings of the National Academy of Sciences of the United States of America*, 110, 52–57.
- Vitasse, Y., Schneider, L., Rixen, C., Christen, D., & Rebetez, M. (2018). Increase in the risk of exposure of forest and fruit trees to spring frosts at higher elevations in Switzerland over the last four decades. *Agricultural and Forest Meteorology*, 248, 60–69.
- Wang, W., Wang, H., Zu, Y., Li, X., & Takayoshi, K. (2006). Characteristics of the temperature coefficient, Q₁₀, for the respiration of non-photosynthetic organs and soils of forest ecosystems. *Frontiers of Forestry in China*, 2, 125–135.
- Yang, J., He, Y., Aubrey, D. P., Zhuang, Q., & Teskey, R. O. (2016). Global patterns and predictors of stem CO₂ efflux in forest ecosystems. *Global Change Biology*, 22, 1433–1444.
- Zhang, X., Friedl, M. A., Schaaf, C. B., Strahler, A. H., Hodges, J. C. F., Gao, F., ... Huete, A. (2003). Monitoring vegetation phenology using MODIS. *Remote Sensing of Environment*, 84, 471–475.
- Zohner, C. M., Mo, L., Renner, S. S., Svenning, J. C., Vitasse, Y., Benito, B. M., ... Crowther, T. W. (2020). Late-spring frost risk between 1959 and 2017 decreased in North America but increased in Europe and Asia. *Proceedings of the National Academy of Sciences*, 117, 12192–12200. <http://dx.doi.org/10.1073/pnas.1920816117>.

SUPPORTING INFORMATION

Additional supporting information may be found online in the Supporting Information section at the end of this article.

How to cite this article: D'Andrea E, Rezaie N, Prislan P, et al. Frost and drought: Effects of extreme weather events on stem carbon dynamics in a Mediterranean beech forest. *Plant Cell Environ*. 2020;1–15. <https://doi.org/10.1111/pce.13858>